

Article

# Synthesis and Crosslinking of Polyether-Based Main Chain Benzoxazine Polymers and Their Gas Separation Performance

Muntazim Munir Khan, Karabi Halder, Sergey Shishatskiy and Volkan Filiz \*

Helmholtz-Zentrum Geesthacht, Institute of Polymer Research, Max-Planck-Strasse 1, 21502 Geesthacht, Germany; muntazim.khan@hzg.de (M.M.K.); karabi.halder@hzg.de (K.H.); sergey.shishatskiy@hzg.de (S.S.)

\* Correspondence: volkan.filiz@hzg.de; Tel.: +49-41-5287-2425

Received: 28 December 2017; Accepted: 22 February 2018; Published: 23 February 2018

**Abstract:** The poly(ethylene glycol)-based benzoxazine polymers were synthesized via a polycondensation reaction between Bisphenol-A, paraformaldehyde, and poly(ether diamine)/Jeffamine<sup>®</sup>. The structures of the polymers were confirmed by proton nuclear magnetic resonance spectroscopy (<sup>1</sup>H-NMR), indicating the presence of a cyclic benzoxazine ring. The polymer solutions were casted on the glass plate and cross-linked via thermal treatment to produce tough and flexible films without using any external additives. Thermal properties and the crosslinking behaviour of these polymers were studied by thermogravimetric analysis (TGA) and differential scanning calorimetry (DSC). Single gas (H<sub>2</sub>, O<sub>2</sub>, N<sub>2</sub>, CO<sub>2</sub>, and CH<sub>4</sub>) transport properties of the crosslinked polymeric membranes were measured by the time-lag method. The crosslinked PEG-based polybenzoxazine membranes show improved selectivities for CO<sub>2</sub>/N<sub>2</sub> and CO<sub>2</sub>/CH<sub>4</sub> gas pairs. The good separation selectivities of these PEG-based polybenzoxazine materials suggest their utility as efficient thin film composite membranes for gas and liquid membrane separation technology.

**Keywords:** benzoxazine; polycondensation; membranes; gas transport properties; Jeffamine<sup>®</sup>

## 1. Introduction

Membrane-based gas separation has attracted significant interest in the industrial sector due to its advantages over conventional separation methods. Polymeric materials are promising candidates for fabricating membranes due to their high competitiveness in performance and cost efficiency [1]. Although a vast number of materials have been reported, only a few polymeric materials have been used for industrial membrane-based separations (e.g., O<sub>2</sub>/N<sub>2</sub>, CO<sub>2</sub>/N<sub>2</sub>, CO<sub>2</sub>/CH<sub>4</sub>) [2]. The accomplishment of high-efficiency gas separation requires high performance membranes that possess both good permeability and permselectivity. However, there exists a trade-off between gas permeability and permselectivity, described by the Robeson upper-bound relationship [3].

Poly(ethylene glycol) (PEG) containing polymers have been extensively studied as membrane materials for CO<sub>2</sub> separation from permanent gases. CO<sub>2</sub> was highly soluble in PEG due to the quadrupole moment resulting in favourable intermolecular interactions with polar (ether) groups in polymers, where the diffusion of CO<sub>2</sub> and other gases was relatively high and did not influence the selectivity because of the PEGs' rubbery nature, leading to enhanced gas permeability and solubility selectivity [4–6]. In addition, hetero-aromatic polymers like polyimides and polyamides show specific physicochemical properties, such as a high value of gas pair selectivity (e.g., CO<sub>2</sub>/N<sub>2</sub> or CO<sub>2</sub>/CH<sub>4</sub>) in gas separation, which make them promising materials for membrane technology applications [7–9]. Likely, oxazine, which is also a member of N-containing organic heterocyclic, is a favourable structure in a polymer membrane for CO<sub>2</sub> separation. A common type of oxazine ring is 1,3-benzoxazine, which receives considerable attention in academia and the chemical industry.

Benzoxazine polymerization has many distinct properties such as negligible volume shrinkage upon curing, does not require any harsh acid catalyst or additives for curing, high thermal stability, low water absorption, and high char-yield of the cured products [10–13]. Additionally, benzoxazines also have immense molecular design flexibility, which allows them to be tailored to a particular application simply by substituting different functionalities into the primary amine or phenolic reactants [14]. An area of benzoxazine research has been developed where polymeric benzoxazines were synthesized by replacing the starting monofunctional amines reactant (or monofunctional phenols) of classical monomeric benzoxazines with difunctional phenols (or difunctional amines) [15–17]. The resulting polymer with repeating benzoxazine units in the main chain is formed. At this point, the benzoxazine acts like an ordinary thermoplastic, which has good solubility, processability, and film formation properties. Upon curing at an elevated temperature, this thermoplastic polymer can be crosslinked via thermally activated ring-opening polymerization (ROP) of the oxazine ring in the main polymer chain. Thus, this thermoplastic/thermosetting crossover molecule gives the advantage of thermoplastic processability with thermosetting polymer characteristics. Good dimensional stability, creep resistance, and great thermal and chemical resistance were some of the common advantages of thermosetting polymers that were observed in cross-linked mainchain-type polybenzoxazines [18,19].

In this study, we report on the preparation of the PEG-based polybenzoxazine from Bisphenol A, aliphatic poly(ether diamine), in the presence of paraformaldehyde. The polymer structure was cured via thermally activated ring-opening polymerization (ROP). The crosslinked films were characterized by differential scanning calorimetry (DSC), thermogravimetric analysis (TGA), and gas-separation techniques.

## 2. Materials and Methods

### 2.1. Materials

Poly(ether diamine)s or Jeffamine<sup>®</sup> of different molecular weights (95%) were kindly supplied by Huntsman. The chemical structure, composition, and molecular weight of Jeffamine<sup>®</sup> are shown in Table 1.

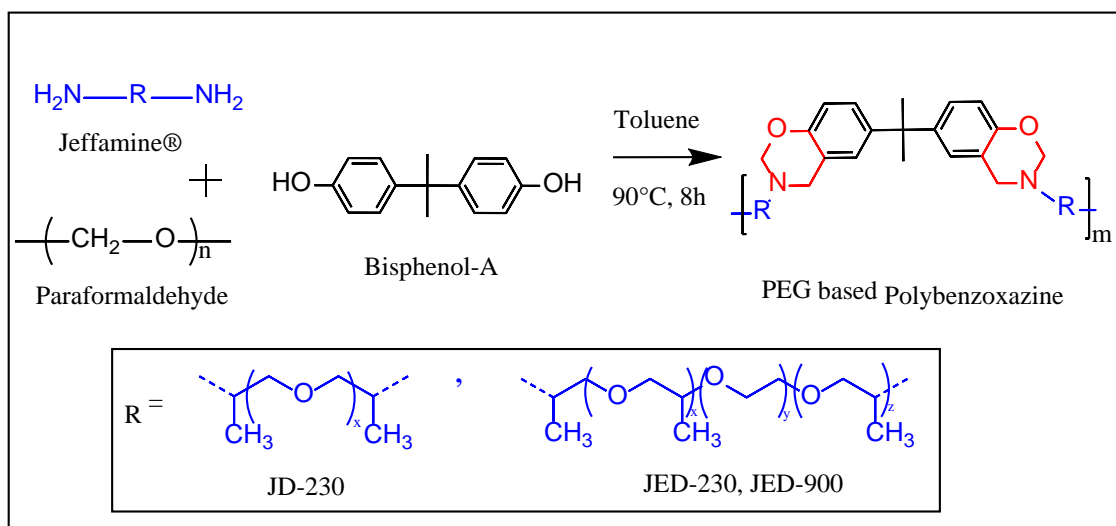
**Table 1.** Chemical structure, composition, and molecular weights of Jeffamine<sup>®</sup> used for polymer synthesis.

Commercial Name	Code	Chain Architecture		Molecular Weight (g/mol)
		x		
Jeffamine <sup>®</sup> D-230	JD230	~2.5		230
Jeffamine <sup>®</sup> D structure				
Jeffamine <sup>®</sup> ED-600	JED600	y ~9	x + z ~3.6	600
Jeffamine <sup>®</sup> ED-900	JED900	~12.5	~6	900
Jeffamine <sup>®</sup> ED structure				

Bisphenol-A (>99%), paraformaldehyde (96%) were used as purchased from Aldrich (St. Louis, MO, USA). Toluene (~99%) and hexane (~99%) were used as purchased from Merck (Kenilworth, NJ, USA).

## 2.2. Synthesis of PEG-Based Main Chain Benzoxazine Polymer

All polymer synthesis followed the same procedure: an equimolar mixture of Jeffamine<sup>®</sup> (1 mol) and Bisphenol-A (1 mol), and paraformaldehyde (4 mol) in toluene (20% solid content) was stirred with magnetic stirring at 90 °C for 8 h, according to Scheme 1.



**Scheme 1.** Synthesis of PEG-based main-chain polybenzoxazine.

The reaction mixture was allowed to cool to room temperature, followed by the evaporation of toluene by distillation under high pressure. The resulting viscous, transparent yellow compound was washed in hexane five times (each 100 mL) and dried under vacuum for 48 h at room temperature. The polymer designations were poly(BZ-JD) and poly(BZ-JED). In order to indicate the particular structure of the Jeffamine<sup>®</sup>, molecular weight information was added; e.g., poly(BZ-JD230), poly(BZ-JED600), and poly(BZ-JED900) indicate molecular weights of 230, 600, and 900, respectively.

## 2.3. Crosslinking of PEG-Based Main Chain Benzoxazine Polymer

The polymers were dissolved in toluene (20 wt %). A film was cast over a levelled hydrophobic glass plate to prevent surface adhesion. Toluene was evaporated first at 60 °C for 12 h and then in a convection oven at 90 °C for 24 h. Cross-linking took place in a convection oven at 200 °C for 5 h and gave brown transparent polymer films. The temperature was gradually increased from 120 to 200 °C in intervals of 20 °C. The temperature steps were maintained for 2 h until a constant value was attained.

## 2.4. Characterization

### 2.4.1. Proton Nuclear Magnetic Resonance (<sup>1</sup>H-NMR)

NMR spectra were recorded on a Bruker AV300 NMR spectrometer (Bruker Biospin GmbH, Karlsruhe, Germany) operating at a field of 7 Tesla (300 MHz) using a 5 mm <sup>1</sup>H TXI probe and a sample temperature of 298 K. <sup>1</sup>H spectra were recorded applying a 10 ms 90° pulse.

### 2.4.2. Differential Scanning Calorimetry (DSC)

DSC experiments were performed in a DSC1 (Starysystem) from Mettler Toledo, Gießen, Germany, using a nitrogen purge gas stream (60 mL/min) at a scan rate of 10 K/min. Heating and cooling scans were performed by initially heating the sample up to 150 °C and holding it at that temperature for 5 min in order to erase previous thermal history, if any, and the sample was then cooled down to 30 °C.

Finally, a second heating scan up to 300 °C and a second cooling scan down to 30 °C was applied. The DSC thermograms presented here correspond to the second heating.

#### 2.4.3. Thermalgravimetric Analysis (TGA)

Thermogravimetric analysis (TGA) was used to investigate the onset degradation temperature and the measurements were obtained using a Netzsch TG209 F1 Iris instrument (NETZSCH-Gerätebau GmbH, Selb, Germany) under argon flow (20 mL min<sup>-1</sup>) from 25 to 900 °C at 10 K/min.

#### 2.4.4. Gas Separation Measurement

Permeabilities of four pure gases (H<sub>2</sub>, N<sub>2</sub>, O<sub>2</sub>, CO<sub>2</sub>, and CH<sub>4</sub>) were measured by a pressure increase time-lag apparatus at 30 °C [20–25]. Permeability (*P*), diffusivity (*D*), solubility (*S*), and selectivity ( $\alpha_{i/j}$ ) for gases *i* and *j* were determined under steady state conditions by the following equations:

$$P = D \cdot S = \frac{V_p l (p_{p2} - p_{p1})}{ART \Delta t [p_f - \frac{(p_{p2} + p_{p1})}{2}]} \quad (1)$$

$$D = \frac{l^2}{6\theta} \quad (2)$$

$$\alpha_{i/j} = \frac{P_i}{P_j} = \frac{D_i S_i}{D_j S_j} \quad (3)$$

where *V<sub>p</sub>* was the constant permeate volume, *R* was the gas constant, *l* was the film thickness, *A* was the effective area of the membrane,  $\Delta t$  was the time for the permeate pressure increase from *p<sub>p1</sub>* to *p<sub>p2</sub>*, *p<sub>f</sub>* was the feed pressure, and  $\theta$  was the time-lag. The solution–diffusion transport model [26] was applied for discussing the gas transport properties of polymeric membranes, and the selectivities of membranes for gas “*I*” relative to another gas “*j*” was the ratio of their permeabilities obtained from Equation (3).

### 3. Results and Discussion

#### 3.1. Synthesis and Characterization of PEG-Based Main Chain Benzoxazine Polymer

Main-chain PEG type polybenzoxazines were synthesized via the typical polycondensation reaction of a Jeffamine<sup>®</sup> with a 230, 600, and 900 g/mol molecular weight, Bisphenol-A, and paraformaldehyde [27–31], according to Scheme 1.

The synthesis of PEG-based main-chain polybenzoxazine was dependent on the reaction of Jeffamine<sup>®</sup>, Bisphenol-A, and paraformaldehyde in the molar ratio of 1:1:4. The reaction conditions for the synthesis of poly(BZ-JD230) at the first place were examined. When the mixture was heated at 100 °C for 1 h without solvent (solvent-less method), insoluble bulky solid was obtained, suggesting the difficulties of applying the solvent-less method. Therefore, the solvent method was implemented. When the mixture was refluxed in the solvent (in our case toluene), the formation of gel was greatly decreased.

Different poly(ether diamine) chain length allows for design flexibility of the main chain-PEG type benzoxazine polymer, which consists of repeating units of a bifunctional benzoxazine structure bonded to a relatively large poly(ether diamine)s structure. Moreover, the Jeffamine<sup>®</sup> and Bisphenol-A was a typical amino and phenolic ingredient for benzoxazine synthesis, respectively. Moreover, Bisphenol-A was common reagent for a wide range of commercial polymers, including polyesters, polycarbonates, and various epoxy resins. All of the synthesized polymers were soluble in organic solvents like chloroform, dioxane, dimethylformamide, dimethylacetamide, dimethyl sulfoxide, and toluene. Toluene was a chosen solvent for the synthesis due to good polymer solubility and minimal health concerns. The poly(ethylene glycol) backbone of Jeffamine<sup>®</sup> might cause an enhancement of its solubility in water. As Jeffamine<sup>®</sup> molecular weight increases solubility in water and alcohols increases.

Poly(BZ-JD230) was insoluble in water, slight solubility in water was achieved with poly(BZ-JED600), and complete solubility was observed with poly(BZ-JED900). All of the polymers were viscous liquids at room temperature, the viscosity increasing with Jeffamine<sup>®</sup> molecular weight. The molecular weight ( $M_w$ ) of the PEG-based main-chain polybenzoxazine was in the range of 8000–9000 g/mol with the broad polydispersity (3 to 4), showing that the molecular weight was not so high.

The polymer (PEG-based polybenzoxazine) structure was confirmed by <sup>1</sup>H-NMR spectra. Figure 1a shows the <sup>1</sup>H NMR spectra of Jeffamine<sup>®</sup> (JD230) and Figure 1b shows their corresponding benzoxazine polymer.

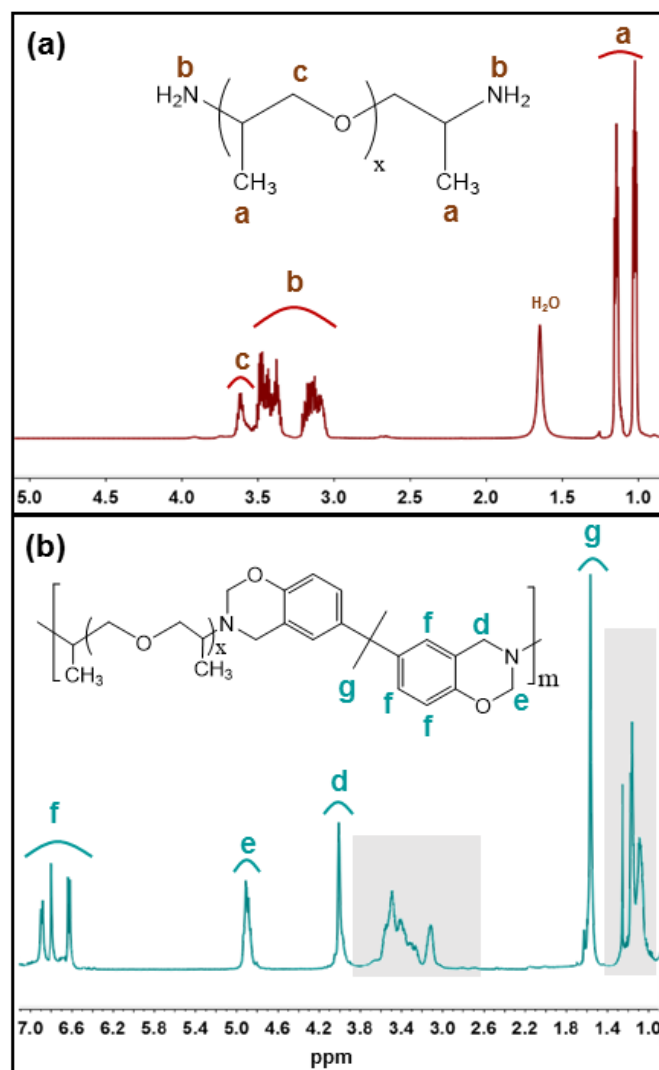


**Figure 1.** <sup>1</sup>H NMR spectra of (a) Jeffamine<sup>®</sup> (JD-230) (b) Jeffamine<sup>®</sup> benzoxazine polymer [Poly(BZ-JD230)].

The peaks at 1.0–1.2 and 3.7 ppm correspond to the  $-\text{CH}_3$  and  $\text{O}-\text{CH}_2-$  groups of the poly(propylene oxide) structure, respectively (Figure 1a). Benzoxazine structure was identified by the presence of the characteristic chemical shifts of the peak of equal integrated intensity due to the methylene groups in the cyclic benzoxazine structure. The peak at 4.0 ppm was due to the protons in  $\text{C}-\text{CH}_2-\text{Ph}$ , and the peak at 4.9 ppm was due to the protons in  $\text{O}-\text{CH}_2-\text{N}$ . The aromatic protons of the benzoxazine structure appear between 6.6 and 7.3 ppm (Figure 1b). The shaded region inside Figure 1b corresponds to the excess proton from Jeffamine<sup>®</sup> (JD230) in the polymer. Polymers synthesized using other Jeffamine<sup>®</sup> (JED600 and JED900) reactants show similar <sup>1</sup>H NMR spectra.

Differential scanning calorimetry (DSC) was used to study the thermal transition of both uncrosslinked and crosslinked PEG-based polybenzoxazine in the temperature range from 50 to 300 °C (Figure 2). The polymer film was first placed at 60 °C for 12 h to remove the solvent. In order to achieve further evaporation of the solvent before the beginning of cross-linking, samples were held at 90 °C for 24 h. Figure 2a depicts the DSC thermograms, illustrating the thermal behaviour of the uncrosslinked polymers. From the DSC results, a single exothermic peak is exhibited, which was due to the ring-opening polymerization (ROP) of the benzoxazine. All exothermic peaks were fairly broad, with total enthalpies of 142, 82, and 66 J/g and exothermic peaks at 241, 245, and 249 °C for poly(BZ-JD230), poly(BZ-JED600), and poly(BZ-JED900), respectively. As PEG length in the polymer was increased, the exothermic heat of polymerization attributed to benzoxazine ring-opening decreased due to a dilution effect [14]. The crosslinked polymers were also characterized by DSC and the results are shown in Figure 2b.

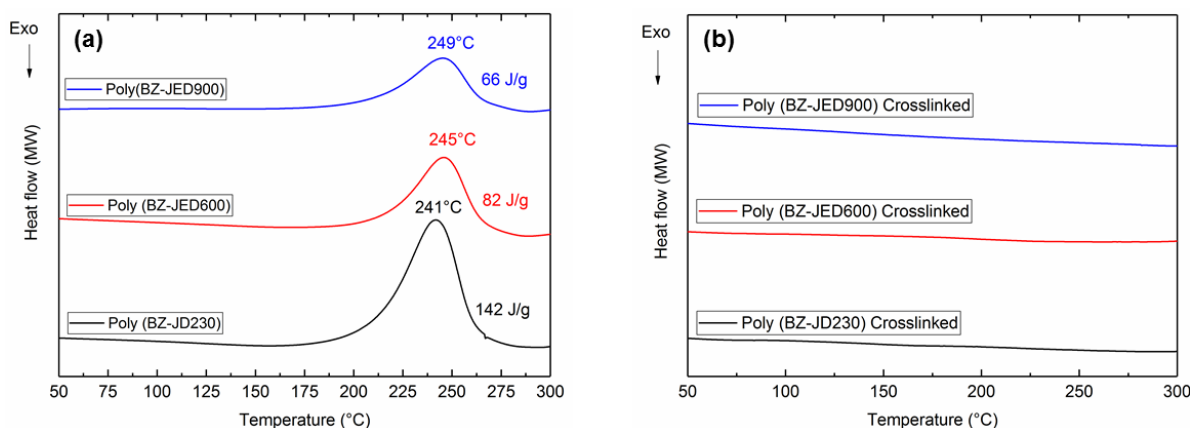


**Figure 2.** DSC thermograms (second heating cycle) of (a) uncrosslinked and (b) crosslinked PEG-based polybenzoxazine.

### 3.2. Characterization of Thermally Crosslinked PEG-Based Main Chain Benzoxazine Polymer

The PEG-based polybenzoxazine materials were dissolved in toluene (20 wt %) and cast on a glass plate. The solvent was removed by drying at 60 °C for 12 h. After heat treatment, brown transparent polybenzoxazine films were obtained. The physical appearance of crosslinked films is shown in Figure 3. All crosslinked polybenzoxazine films were mechanically stable, tough, and ~70–80 μm thick.

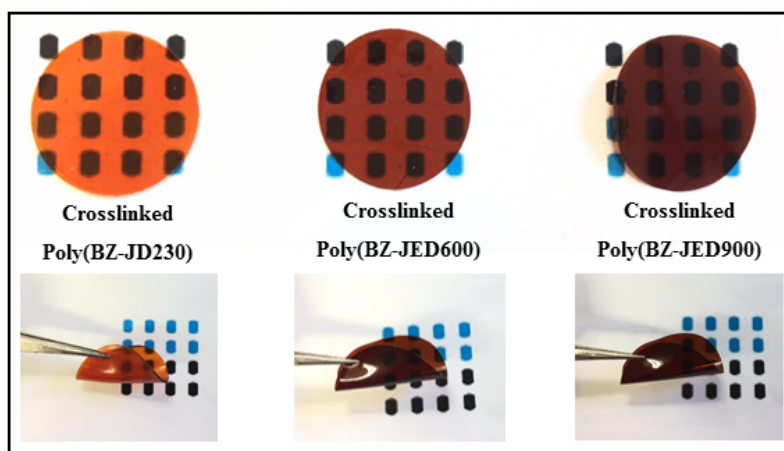


**Figure 3.** Physical appearance of crosslinked polybenzoxazine films.

From the DSC data, it was confirmed that the crosslinking or ROP was observed between 200–270 °C for all PEG-based polybenzoxazine polymers. Therefore, poly(BZ-JD230), poly(BZ-JED600), and poly(BZ-JED900) films were crosslinked at 200 °C for 5 h. In order to check the thermal stability of crosslinked polymers, TGA was carried out under a nitrogen atmosphere and the results are shown in Figure 4.

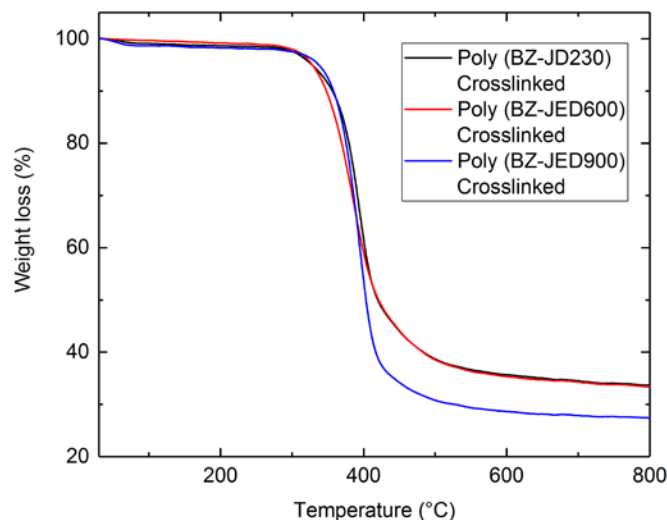


**Figure 4.** TGA of crosslinked PEG-based polybenzoxazine.

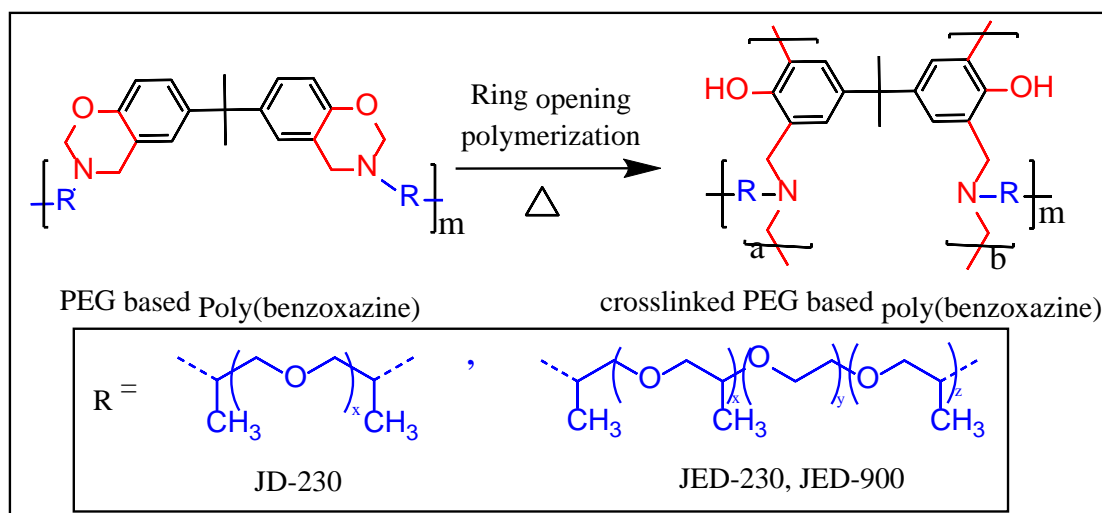
The onset temperature of degradation of the polymers increased with poly(ether diamine) chain length in Jefamine®. The values of 10 wt % weight reduction temperature,  $T_{d10}$ , for poly(BZ-JD230), poly(BZ-JED600), and poly(BZ-JED900) were 340, 350, and 360 °C, respectively. It was possibly related to the C–N bond concentration at the polyether chain/benzoxazine linkage that could have been acting as the thermally weak link. As the polyether chain molecular weight decreases, the concentration of such links increases, which then might lead to the weakening of the thermal stability [32]. A similar case was reported for the main-chain-type polybenzoxazine, where the fluorinated aliphatic chain was connected to the amine group through a  $\text{CH}_2$  group. When this  $\text{CH}_2$  group was replaced with a phenyl group, the thermal stability was drastically enhanced [33]. The char yield at 800 °C increased as poly(ether diamine) length increased. Char yield for poly(BZ-JD230), poly(BZ-JED600), and poly(BZ-JED900) was 4.3, 4.0, and 3.3%, respectively (Table 2). This trend can be attributed to a higher density of benzoxazine cross-linking in the main chain.

**Table 2.** Thermal degradation of PEG-based polybenzoxazine materials.

Polymer	$T_{d10}$ (°C)	Onset Temperature (°C)	Char Yield (%)
Poly(BZ-JD230)	340	370	4.3
Poly(BZ-JED600)	350	380	4.0
Poly(BZ-JED900)	360	390	3.3

The crosslinked polymers were characterized by DSC and the results are shown in Figure 2b. There is a significant exothermic difference between non-crosslinked and crosslinked polymers (Figure 2a,b). The exotherm completely disappears after crosslinking, showing that ring opening of oxazine was completed for all crosslinked polymers.

The crosslinked structure was supported by insolubility in an organic solvent such as tetrahydrofuran, toluene, and chloroform. The possible structure of the PEG-based crosslinked polybenzoxazine is depicted in Scheme 2, according to reference [15].



**Scheme 2.** Predicted crosslinking mechanism of PEG-based polybenzoxazine.

### 3.3. Gas Transport Properties of Crosslinked PEG-Based Main Chain Benzoxazine Polymer

Free standing films of polymers (as shown in Figure 3) for gas separation could be prepared by thermal crosslinking and they were tough enough to allow a measurement of gas permeability, which was not possible for the precursor polymeric films. Single gas permeation for  $H_2$ ,  $N_2$ ,  $O_2$ ,  $CO_2$ , and  $CH_4$  was carried out at  $30^\circ C$  by the time-lag instrument on crosslinked polymer films. The data on the gas permeability coefficient and the values of ideal permselectivities are shown in Table 3. The order of the gas permeability was  $CO_2 > O_2 > CH_4 > N_2$ .

**Table 3.** Gas separation performance of PEG-based polybenzoxazine.

Polymers	Permeability Coefficient (Barrer <sup>1</sup> )				Permselectivity		
	$O_2$	$N_2$	$CO_2$	$CH_4$	$O_2/N_2$	$CO_2/N_2$	$CO_2/CH_4$
Poly(BZ-JD230)	11	2	55	11	5.4	27.6	4.6
Poly(BZ-JED600)	14	4	128	12	3.4	31.8	11.8
Poly(BZ-JED900)	21	8	345	22	2.7	43.5	15.7

$$^1 \text{ Barrer} = 1 * 10^{-10} \cdot \frac{\text{cm}^3_{\text{STP}} \cdot \text{cm}}{\text{cm}^3 \cdot \text{sec} \cdot \text{cmHg}}$$

Polymers of heteroaromatic structures were characterized by a high level of selectivity but relatively low permeability in the gas separation process [34,35]. It was shown that the permeability coefficient of all gases in Poly(BZ-JD230) was lower than those of gases through the Poly(BZ-JED900) film. The reason for the high permeability of Poly(BZ-JED900) was due to the presence of PEG chains in the crosslinked polymeric membrane. The PEG group has a stronger interaction with a polar gas, such as  $CO_2$ , than a nonpolar gas, e.g.,  $N_2$ . In that case, the polar gas solubility can be enhanced and the gas permeability increased, which facilitates the improvement of the total  $CO_2/N_2$  and  $CO_2/CH_4$  gas pair selectivity [36–39]. The permselectivity of  $CO_2/N_2$  and  $CO_2/CH_4$  for Poly(BZ-JED900) was found to be higher than those of the membrane Poly(BZ-JD230).

Furthermore, the gas permeability tendency of crosslinked polymeric membranes was  $CO_2 > O_2 > CH_4 > N_2$ . This order was the same as for most polymeric rubbery membranes, which follows the solution-diffusion mechanism for the gas permeation. In this direction, the important key parameter determining the permeability coefficient was the critical temperature of the gases [40] [ $CO_2$  (304.2 K) >  $CH_4$  (190.6 K) >  $O_2$  (154.4 K) >  $N_2$  (126.2 K) >  $H_2$  (33.2 K), data according to [41]]. The gases with a higher critical temperature have a higher solubility coefficient and condensability.  $N_2$  with the lowest critical temperature would be expected to have the lowest permeability coefficient.



Figure 5 clearly shows the dependence of the gas solubility coefficient as a function of the critical temperature of gas molecules in crosslinked PEG-based polybenzoxazine polymeric membranes.

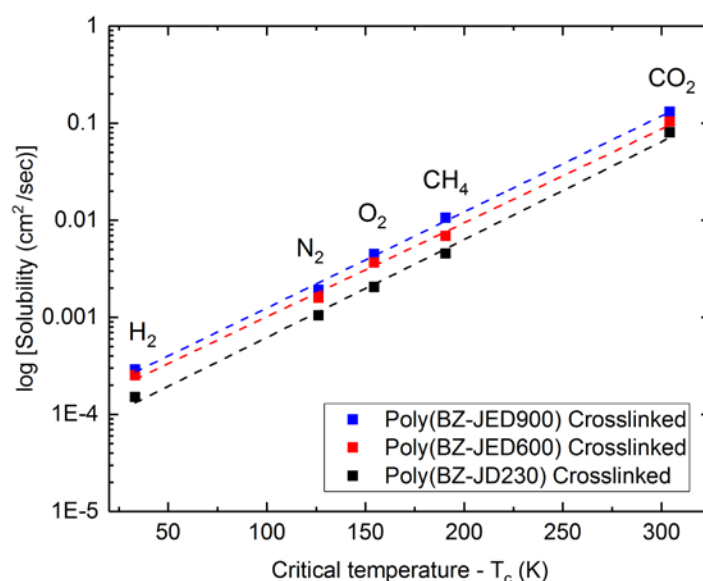


**Figure 5.** Dependence of gas solubility coefficients as a function of critical temperature ( $T_c$ ) of gas molecules for PEG-based polybenzoxazine.

Correlation analysis of the gas permeability parameters of the crosslinked PEG-based polybenzoxazine films was carried out using the Teplyakov method [42], which was based on the dependence of the gas diffusion coefficient,  $D$ , on the effective kinetic diameter of gas molecule,  $d$ , and the Equation can be given as:

$$\log D = K_1 - K_2 \times d^2 \quad (4)$$

where  $K_1$  and  $K_2$  were the constants. Usually, the coefficients of gas diffusion through a polymer depend linearly on the diameter of the gas molecules. Figure 6 shows the correlation dependence of diffusion coefficients on the effective kinetic diameter of gas molecules. The points corresponding to the gas diffusivity ( $\log D$ ) values as a function of effective kinetic diameter ( $d$ ) for the polybenzoxazine films display a distinct deviation from linearity. The deviation from linearity could indicate the presence of some specifics of the polymer structure and excess free volume in the polymer. The order of effective kinetic diameter was  $\text{CH}_4$  (0.318 nm) >  $\text{N}_2$  (0.304 nm) >  $\text{CO}_2$  (0.302 nm) >  $\text{O}_2$  (0.289 nm) >  $\text{H}_2$  (0.214 nm) [43]; however, the smallest kinetic diameter of  $\text{H}_2$  leads to a high diffusion coefficient that makes it more permeable than all other gases except  $\text{CO}_2$ .

In order to see the performance of crosslinked PEG-based polybenzoxazine polymeric materials among known gas-separation materials, their transport properties were plotted on a Robeson plot (Figure 7). Robeson analyzed data on permeability and selectivity for a large number of glassy and rubbery polymers and established the position of the upper bound line for several gas pairs in 1991; before redefining them in 2008 [3]. Figure 7 shows the upper bound line for membrane separation of the  $\text{CO}_2/\text{N}_2$  and  $\text{CO}_2/\text{CH}_4$  gas pairs. It was observed that polybenzoxazine polymeric films were located near the Robeson upper bound lines and that the performance of the poly(BZ-JED900) film was better than that of the poly(BZ-JD230) film in the separation of both the  $\text{CO}_2/\text{N}_2$  and  $\text{CO}_2/\text{N}_2$  gas pairs.

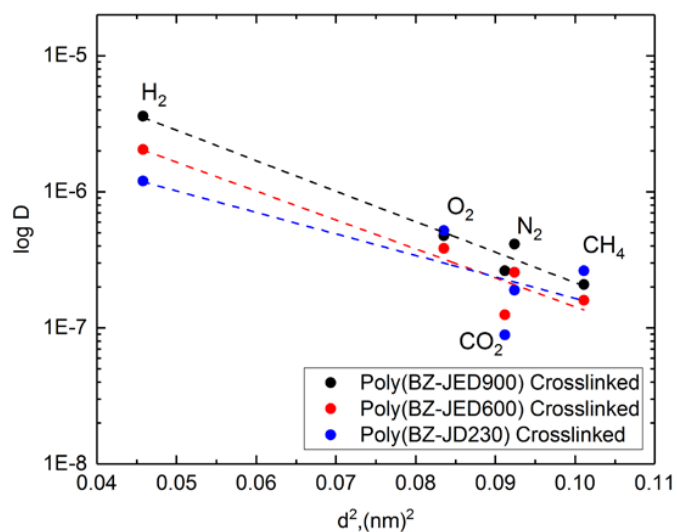


**Figure 6.** Dependence of gas diffusivity coefficients as a function of effective kinetic diameter of gas molecules for PEG-based polybenzoxazine.

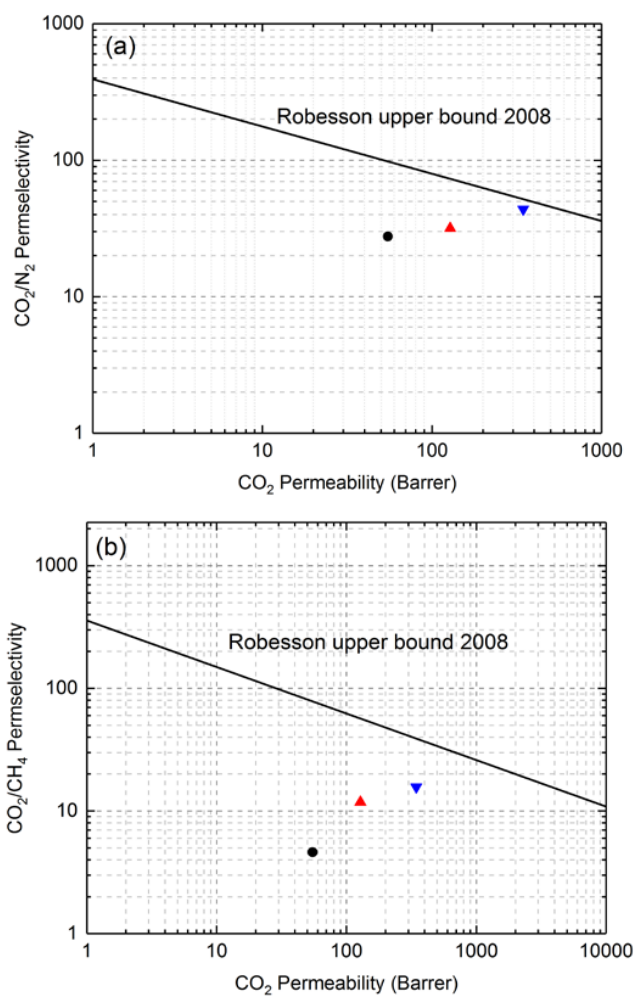


**Figure 7.** Robeson plot for (a) CO<sub>2</sub>/N<sub>2</sub> and (b) CO<sub>2</sub>/CH<sub>4</sub> gas pair showing data for PEG-based polybenzoxazine films measured at 30°C. [●—Poly(BZ-JD230), ▲—Poly(BZ-JED600), and ▼—Poly(BZ-JED900)].

#### 4. Conclusions

The poly(ethylene glycol)-based polybenzoxazine precursor containing a cyclic benzoxazine group in the backbone was synthesized successfully by a polycondensation reaction between Bisphenol-A, paraformaldehyde, and poly(ether diamine) known as Jeffamine<sup>®</sup>. The precursor polymer solutions were cast on a glass plate and crosslinked via thermally activated ring opening polymerization of the cyclic benzoxazine structure. The flexible and mechanically stable polymer films were obtained without using any external initiators, accelerators, catalysts, or reactive diluents. These crosslinked polymers films were characterized by DSC and TGA. Gas permeation of the crosslinked films was measured using single gas H<sub>2</sub>, O<sub>2</sub>, N<sub>2</sub>, CO<sub>2</sub>, and CH<sub>4</sub>. The gas permeability and permselectivity (CO<sub>2</sub>/N<sub>2</sub> and CO<sub>2</sub>/CH<sub>4</sub> gas pairs) of polybenzoxazine polymers increases as the PEG chain length increases on polybenzoxazine. Correlation analysis of gas diffusion showed a linearity in crosslinked films. The position of these crosslinked PEG-based polybenzoxazine films on the Robeson plot was close to the upper bound line for the CO<sub>2</sub>/N<sub>2</sub> and CO<sub>2</sub>/CH<sub>4</sub> gas pairs. The unique feature of this class of materials provides the possibility of preparing efficient thin film composite membranes for various gas and liquid membrane separation applications.

**Acknowledgments:** The authors thank Silvio Neumann for the TGA, DSC, and spectroscopic analysis. This work was financially supported by the Helmholtz Association of German Research Centres through the project Helmholtz Portfolio MEM-BRAIN.

**Author Contributions:** Muntazim Munir Khan carried out the experiments and drafted the manuscript. Karabi Halder was involved in scientific discussions. Volkan Filiz supervised the study and Sergey Shishatskiy was involved in scientific discussions. All authors read and approved the final manuscript.

**Conflicts of Interest:** The authors declare that they have no conflicts of interest.

#### References

1. Pandey, P.; Chauhan, R.S. Membranes for gas separation. *Prog. Polym. Sci.* **2001**, *26*, 853–893. [[CrossRef](#)]
2. Baker, R.W. Overview of membrane science and technology. In *Membrane Technology and Applications*; John Wiley & Sons, Ltd.: Chichester, UK, 2004; pp. 1–14.
3. Robeson, L.M. The upper bound revisited. *J. Membr. Sci.* **2008**, *320*, 390–400. [[CrossRef](#)]
4. Charmette, C.; Sanchez, J.; Gramain, P.; Masquelez, N. Structural characterization of poly(ethylene oxide-co-epichlorohydrin) membranes and relation with gas permeation properties. *J. Membr. Sci.* **2009**, *344*, 275–280. [[CrossRef](#)]
5. Rahman, M.M.; Filiz, V.; Shishatskiy, S.; Abetz, C.; Neumann, S.; Bolmer, S.; Khan, M.M.; Abetz, V. Pebax<sup>®</sup> with peg functionalized POSS as nanocomposite membranes for CO<sub>2</sub> separation. *J. Membr. Sci.* **2013**, *437*, 286–297. [[CrossRef](#)]
6. Lin, H.; Van Wagner, E.; Freeman, B.D.; Toy, L.G.; Gupta, R.P. Plasticization-enhanced hydrogen purification using polymeric membranes. *Science* **2006**, *311*, 639–642. [[CrossRef](#)] [[PubMed](#)]
7. Tena, A.; Rangou, S.; Shishatskiy, S.; Filiz, V.; Abetz, V. Claisen thermally rearranged (CTR) polymers. *Sci. Adv.* **2016**, *2*. [[CrossRef](#)] [[PubMed](#)]
8. Polotskaya, G.; Guliy, N.; Goikhman, M.; Podeshvo, I.; Brozova, L.; Pientka, Z. Structure and gas transport properties of polybenzoxazinoneimides with biquinoline units in the backbone. *Macromol. Symp.* **2015**, *348*, 44–53. [[CrossRef](#)]
9. Matteucci, S.; Yampolskii, Y.; Freeman, B.D.; Pinnau, I. Transport of gases and vapors in glassy and rubbery polymers. In *Materials Science of Membranes for Gas and Vapor Separation*; John Wiley & Sons, Ltd.: Chichester, UK, 2006; pp. 1–47.
10. Demir, K.D.; Tasdelen, M.A.; Uyar, T.; Kawaguchi, A.W.; Sudo, A.; Endo, T.; Yagci, Y. Synthesis of polybenzoxazine/clay nanocomposites by in situ thermal ring-opening polymerization using intercalated monomer. *J. Polym. Sci. Part A Polym. Chem.* **2011**, *49*, 4213–4220. [[CrossRef](#)]
11. Dogan Demir, K.; Kiskan, B.; Yagci, Y. Thermally curable acetylene-containing main-chain benzoxazine polymers via Sonogashira coupling reaction. *Macromolecules* **2011**, *44*, 1801–1807. [[CrossRef](#)]

12. Agag, T.; Geiger, S.; Ishida, H. Chapter 13-thermal properties enhancement of polybenzoxazines: The role of additional non-benzoxazine polymerizable groups. In *Handbook of Benzoxazine Resins*; Elsevier: Amsterdam, The Netherlands, 2011; pp. 263–286.
13. Hacaloğlu, J.; Uyar, T.; Ishida, H. Chapter 14-thermal degradation mechanisms of polybenzoxazines. In *Handbook of Benzoxazine Resins*; Elsevier: Amsterdam, The Netherlands, 2011; pp. 287–305.
14. Agag, T.; Geiger, S.; Alhassan, S.M.; Qutubuddin, S.; Ishida, H. Low-viscosity polyether-based main-chain benzoxazine polymers: Precursors for flexible thermosetting polymers. *Macromolecules* **2010**, *43*, 7122–7127. [[CrossRef](#)]
15. Takeichi, T.; Kano, T.; Agag, T. Synthesis and thermal cure of high molecular weight polybenzoxazine precursors and the properties of the thermosets. *Polymer* **2005**, *46*, 12172–12180. [[CrossRef](#)]
16. Yeganeh, H.; Razavi-Nouri, M.; Ghaffari, M. Investigation of thermal, mechanical, and electrical properties of novel polyurethanes/high molecular weight polybenzoxazine blends. *Polym. Adv. Technol.* **2008**, *19*, 1024–1032. [[CrossRef](#)]
17. Kiskan, B.; Yagci, Y.; Sahmetlioglu, E.; Toppare, L. Preparation of conductive polybenzoxazines by oxidative polymerization. *J. Polym. Sci. Part A Polym. Chem.* **2007**, *45*, 999–1006. [[CrossRef](#)]
18. Nagai, A.; Kamei, Y.; Wang, X.-S.; Omura, M.; Sudo, A.; Nishida, H.; Kawamoto, E.; Endo, T. Synthesis and crosslinking behavior of a novel linear polymer bearing 1,2,3-triazol and benzoxazine groups in the main chain by a step-growth click-coupling reaction. *J. Polym. Sci. Part A Polym. Chem.* **2008**, *46*, 2316–2325. [[CrossRef](#)]
19. Wang, L.; Gong, W.; Zheng, S. Poly(hydroxyether of bisphenol A)-alt-polydimethylsiloxane: A novel thermally crosslinkable alternating block copolymer. *Polym. Int.* **2009**, *58*, 124–132. [[CrossRef](#)]
20. Khan, M.M.; Filiz, V.; Bengtson, G.; Shishatskiy, S.; Rahman, M.M.; Lillepaerg, J.; Abetz, V. Enhanced gas permeability by fabricating mixed matrix membranes of functionalized multiwalled carbon nanotubes and polymers of intrinsic microporosity (PIM). *J. Membr. Sci.* **2013**, *436*, 109–120. [[CrossRef](#)]
21. Khan, M.M.; Bengtson, G.; Neumann, S.; Rahman, M.M.; Abetz, V.; Filiz, V. Synthesis, characterization and gas permeation properties of anthracene maleimide-based polymers of intrinsic microporosity. *RSC Adv.* **2014**, *4*, 32148–32160. [[CrossRef](#)]
22. Rahman, M.M.; Filiz, V.; Khan, M.M.; Gacal, B.N.; Abetz, V. Functionalization of POSS nanoparticles and fabrication of block copolymer nanocomposite membranes for CO<sub>2</sub> separation. *React. Funct. Polym.* **2015**, *86*, 125–133. [[CrossRef](#)]
23. Koschine, T.; Rätzke, K.; Faupel, F.; Khan, M.M.; Emmmler, T.; Filiz, V.; Abetz, V.; Ravelli, L.; Egger, W. Correlation of gas permeation and free volume in new and used high free volume thin film composite membranes. *J. Polym. Sci. Part B Polym. Phys.* **2015**, *53*, 213–217. [[CrossRef](#)]
24. Khan, M.; Filiz, V.; Emmmler, T.; Abetz, V.; Koschine, T.; Rätzke, K.; Faupel, F.; Egger, W.; Ravelli, L. Free volume and gas permeation in anthracene maleimide-based polymers of intrinsic microporosity. *Membranes* **2015**, *5*, 214. [[CrossRef](#)] [[PubMed](#)]
25. Halder, K.; Khan, M.M.; Grünauer, J.; Shishatskiy, S.; Abetz, C.; Filiz, V.; Abetz, V. Blend membranes of ionic liquid and polymers of intrinsic microporosity with improved gas separation characteristics. *J. Membr. Sci.* **2017**, *539*, 368–382. [[CrossRef](#)]
26. Wijmans, J.G.; Baker, R.W. The solution-diffusion model: A review. *J. Membr. Sci.* **1995**, *107*, 1–21. [[CrossRef](#)]
27. Ning, X.; Ishida, H. Phenolic materials via ring-opening polymerization: Synthesis and characterization of bisphenol-a based benzoxazines and their polymers. *J. Polym. Sci. Part A Polym. Chem.* **1994**, *32*, 1121–1129. [[CrossRef](#)]
28. Kiskan, B.; Yagci, Y.; Ishida, H. Synthesis, characterization, and properties of new thermally curable polyetheresters containing benzoxazine moieties in the main chain. *J. Polym. Sci. Part A Polym. Chem.* **2008**, *46*, 414–420. [[CrossRef](#)]
29. Demir, K.D.; Kiskan, B.; Latthe, S.S.; Demirel, A.L.; Yagci, Y. Thermally curable fluorinated main chain benzoxazine polyethers via Ullmann coupling. *Polym. Chem.* **2013**, *4*, 2106–2114. [[CrossRef](#)]
30. Liu, J.; Ishida, H. Anomalous isomeric effect on the properties of bisphenol f-based benzoxazines: Toward the molecular design for higher performance. *Macromolecules* **2014**, *47*, 5682–5690. [[CrossRef](#)]
31. Sini, N.K.; Azechi, M.; Endo, T. Synthesis and properties of spiro-centered benzoxazines. *Macromolecules* **2015**, *48*, 7466–7472.

32. Hemvichian, K.; Laobuthee, A.; Chirachanchai, S.; Ishida, H. Thermal decomposition processes in polybenzoxazine model dimers investigated by tga-ftir and gc-ms. *Polym. Degrad. Stab.* **2002**, *76*, 1–15. [[CrossRef](#)]
33. Ergin, M.; Kiskan, B.; Gacal, B.; Yagci, Y. Thermally curable polystyrene via click chemistry. *Macromolecules* **2007**, *40*, 4724–4727. [[CrossRef](#)]
34. Koros, W.J.; Fleming, G.K. Membrane-based gas separation. *J. Membr. Sci.* **1993**, *83*, 1–80. [[CrossRef](#)]
35. Wind, J.D.; Paul, D.R.; Koros, W.J. Natural gas permeation in polyimide membranes. *J. Membr. Sci.* **2004**, *228*, 227–236. [[CrossRef](#)]
36. Khan, M.M.; Bengtson, G.; Shishatskiy, S.; Gacal, B.N.; Mushfequr Rahman, M.; Neumann, S.; Filiz, V.; Abetz, V. Cross-linking of polymer of intrinsic microporosity (pim-1) via nitrene reaction and its effect on gas transport property. *Eur. Polym. J.* **2013**, *49*, 4157–4166. [[CrossRef](#)]
37. Rahman, M.M.; Filiz, V.; Shishatskiy, S.; Abetz, C.; Georgopoulos, P.; Khan, M.M.; Neumann, S.; Abetz, V. Influence of poly(ethylene glycol) segment length on CO<sub>2</sub> permeation and stability of polyactive membranes and their nanocomposites with peg poss. *ACS Appl. Mater. Interfaces* **2015**, *7*, 12289–12298. [[CrossRef](#)] [[PubMed](#)]
38. Khan, M.M.; Filiz, V.; Bengtson, G.; Shishatskiy, S.; Rahman, M.; Abetz, V. Functionalized carbon nanotubes mixed matrix membranes of polymers of intrinsic microporosity for gas separation. *Nanoscale Res. Lett.* **2012**, *7*, 504. [[CrossRef](#)] [[PubMed](#)]
39. Lilleparg, J.; Georgopoulos, P.; Emmeler, T.; Shishatskiy, S. Effect of the reactive amino and glycidyl ether terminated polyethylene oxide additives on the gas transport properties of Pebax[registered sign] bulk and thin film composite membranes. *RSC Adv.* **2016**, *6*, 11763–11772. [[CrossRef](#)]
40. Xie, H.; Simha, R. Theory of solubility of gases in polymers. *Polym. Int.* **1997**, *44*, 348–355. [[CrossRef](#)]
41. Lin, H.; Wagner, E.V.; Swinnea, J.S.; Freeman, B.D.; Pas, S.J.; Hill, A.J.; Kalakkunnath, S.; Kalika, D.S. Transport and structural characteristics of crosslinked poly(ethylene oxide) rubbers. *J. Membr. Sci.* **2006**, *276*, 145–161. [[CrossRef](#)]
42. Malykh, O.V.; Golub, A.Y.; Teplyakov, V.V. Polymeric membrane materials: New aspects of empirical approaches to prediction of gas permeability parameters in relation to permanent gases, linear lower hydrocarbons and some toxic gases. *Adv. Colloid Interface Sci.* **2011**, *164*, 89–99. [[CrossRef](#)] [[PubMed](#)]
43. Teplyakov, V.; Meares, P. Correlation aspects of the selective gas permeabilities of polymeric materials and membranes. *Gas Sep. Purif.* **1990**, *4*, 66–74. [[CrossRef](#)]



© 2018 by the authors. Licensee MDPI, Basel, Switzerland. This article is an open access article distributed under the terms and conditions of the Creative Commons Attribution (CC BY) license (<http://creativecommons.org/licenses/by/4.0/>).